Dynamics and adsorption sites for guest molecules in methyl chloride hydrate

2008 J. Phys.: Condens. Matter 20 125219

(http://iopscience.iop.org/0953-8984/20/12/125219)

J. Phys.: Condens. Matter **20** (2008) 125219 (6pp) doi:10.1088/0953-8984/20/12/125219

Dynamics and adsorption sites for guest molecules in methyl chloride hydrate

M Prager[1,2], A Desmedt[3], T Unruh[4] and J Allgaier[1]

[1] Institut für Festkörperforschung, Forschungszentrum Jülich, D-52425 Jülich, Germany
[2] Jülich Center for Neutron Science JCNS, Lichtenbergstraße 4, D-85747 Garching, Germany
[3] LPCM, Université de Bordeaux 1, Talence, France
[4] Technische Universität München, FRM2, D-85747 Garching, Germany

Received 7 December 2007, in final form 5 February 2008
Published 3 March 2008
Online at stacks.iop.org/JPhysCM/20/125219

Abstract
Methyl rotational tunneling, quasielastic spectra and phonon densities of states measured with neutrons at energy transfers from 35 μeV to 40 meV are used to characterize the adsorption sites and potentials of CH_3Cl guest molecules in the two kinds of cages of cubic I methyl chloride hydrate. The model of adsorption to hydrogen bonds of the ice cage explains the broad tunnel spectrum as a superposition of four bands. Up to a temperature $T \sim 80$ K the quasielastic scattering is influenced by quantum motion. Only above $T \sim 80$ K does the effective linewidth follow an Arrhenius behavior with an average activation energy. Rotational potentials contain a significant sixfold component supporting the proposed adsorption to hydrogen bonds with their mirror symmetry. Positional disorder of protons in the hydrogen bonds of the host ice lattice leads to potential distributions of large relative widths $\frac{\delta V}{V} \leqslant 0.35$.

(Some figures in this article are in colour only in the electronic version)

1. Introduction

Partly due to the discovery of methane clathrate as one of the largest energy reservoirs on Earth [1] inclusion compounds have gained new interest. Beside the natural gas hydrates many other molecules can form host–guest structures in an ever increasing variety of inclusion compounds [2, 3]. In hydrates the cages of the water host molecules are only stable if they are—at least partly—filled by guest molecules. A single face of a polyhedral cage is formed by closed rings of 5, 6 or 4 water molecules. These structural units are linked together at their edges. The final three-dimensional body can be characterized by the type and number of polygons forming the surface. Using this convention the cage with 12 pentagon faces, the pentagondodecahedron, is named 5^{12}. To fill the three-dimensional space different kinds of cages have to be combined. The cubic I structure contains two 5^{12} cages and as the second type six $5^{12}6^2$ cages with hexagons forming the top and bottom faces while the sides are closed by pentagons [4, 5].

Rotational barriers of molecular solids are determined by the fundamental intermolecular interaction potentials. They determine the rotational tunnel splittings of librational modes and the frequencies of jump reorientation. Neutron spectroscopy can explore well the two phenomena. A specific motion in clathrates is translation of the whole molecule in the cages of the host lattice, called 'rattling'. It is found in methane hydrate [6–8], methyl iodide hydrate [9] and other inclusion compounds [10].

A well-known property characteristic of hydrates is the location of hydrogen in the network of hydrogen bonds according to ice rules in the presence of Bjerrum defects. The resulting disorder is reflected in an inhomogeneous broadening of rotor transitions [11]. It makes the data analysis more difficult on one hand, while on the other it contains interesting information about one of the most fundamental properties of hydration shells [15].

Our interest is focused on guest molecules containing methyl groups. The simplest such molecules are the methyl halides. According to the literature [12] the three light methyl halide hydrates $CH_3X * 5.75D_2O$ with X = F, Cl or Br assume cubic I crystal structure as methane hydrate. The larger methyl iodide guest molecules require larger cages and hence $CH_3I * 17D_2O$ crystallizes in cubic II structure with eight $5^{12}6^4$ and sixteen 5^{12} cages [12]. In cubic II hydrate the 5^{12} cages are too small to host CH_3I guest molecules.

The methyl halide hydrates were shown [9, 13, 14] to manifest quantum rotation of the CH_3 groups, similarly to the methane hydrate case [11]. In the case of methyl

iodide clathrate [9] new information on the complex potential surface of the $5^{12}6^4$ cage could be obtained from neutron tunneling spectroscopy: three different adsorption sites could be identified. Spin conversion times of the guest molecules depended on the adsorption site and were related to tunneling dynamics of the protons in the water cage, the fastest being on a timescale of hours. This first study was extended to other methyl halide hydrates [13, 14] to test the originally developed model. In the present study, results on $CH_3Cl * 5.75H_2O$ are presented.

2. Theoretical background

The theory of single-particle rotation [16, 17] is the basis of data analysis and was outlined in the previous publications on the same subject [9, 13, 14]. At low temperature rotational tunneling leads to inelastic bands at energies lower than the rotational constant of the methyl group $B = 655$ μeV. At higher temperature rotational diffusion in weak potentials [18] or jump reorientation in stronger ones [19] leads to quasielastic scattering. At increased temperature, rattling in the cage can add another component to the spectra. The inequivalency of structurally different methyl groups and disorder lead to a superposition of different such contributions resulting in complex spectra.

3. Experimental details

3.1. Sample preparation

Methyl chloride of 99.5% purity was obtained from the Aldrich company. At a temperature $T = 20\,^{\circ}$C methyl chloride is a gas with a vapor pressure of ∼12 bar and water is a liquid. To get the stoichiometric mixture of the two constituents a defined quantity of water was transferred into the reaction vessel. Thereafter it was frozen and methyl chloride from a gas reservoir was liquefied into this same volume until the molar ratio of 1:5.75 was reached. The pressure resistant reaction vessel was then sealed and warmed up to room temperature where both constituents are liquids under the CH_3Cl gas pressure. Despite CH_3Cl being insoluble in water, a solution on a molecular level can be obtained under permanent mechanical mixing. This preparation procedure is based on the principles established for synthesizing methyl iodide clathrate [20]. During the stirring procedure the sample was slowly cooled down until the alloy suddenly solidified. The melting point of the new compound, the methyl chloride hydrate, is $T_m \sim 16\,^{\circ}$C. The cold reaction product was then removed from the pressure resistant reaction vessel in a dry argon atmosphere. The lack of pressure when opening the vessel showed that all methyl chloride is bound in the new compound. From the original stoichiometry we conclude that the final product really has the cubic I crystal structure.

3.2. Inelastic neutron scattering

The sample was studied by neutron spectroscopy in the energy range from 35 μeV to 40 meV. Ground state tunnel splittings and stochastic jump processes were investigated using the cold time-of-flight (TOF) spectrometer TOFTOF [21] at the research reactor FRM-II of the Technical University of Munich with energy resolutions from $\delta E = 35$ to 240 μeV. Quasielastic and inelastic spectra shown in the following represent the sums over 30° at an average scattering angle $2\Theta = 99°$. On a cold TOF spectrometer deep inelastic intensity is only visible at high sample temperature on the neutron energy gain side.

At low sample temperature the regime of phonons was also explored in the energy loss of the neutrons using the thermal TOF spectrometer SV29 [22] of Forschungszentrum Jülich with energy resolutions $\delta E = 2.0$ and 0.4 meV.

The samples were contained in flat Al sample holders and were oriented at 45° to the beam. The sample had a thickness of 0.5 mm. The powder is assumed to fill the volume to 60%. In this way a scattering probability of ∼12% is calculated. All data were corrected for background and detector efficiency. Fits are the result of convoluting numerically a theoretical spectrum with the measured resolution function determined with a flat vanadium sample of 1 mm thickness also oriented at 45° to the beam.

4. Results and discussion

4.1. Quantum rotation

The precooled sample was quenched from $T = 50$ to 4.2 K within 16 min. Due to the very low heat conductivity of clathrates [23, 10] the temperature sensor may not show the real sample temperature. The quenching procedure is chosen since it leaves excited rotor E-states at a metastable higher population due to site specific and T dependent slow spin conversion times. In previous studies this procedure had led to enhanced fine structure of the spectra compared to a slowly cooled sample and allowed a better modeling. In the present case broad overlapping bands (figure 1) make a model independent description of the observed intensity profile impossible, however. The scattering function used is related to the one applied to $CH_3I * 17D_2O$ hydrate where on the basis of intensities the three observed bands were assigned to adsorption along the three inequivalent hydrogen bonds in the $5^{12}6^4$ cage [9]. In $CH_3Cl * 5.75H_2O$ and the other cubic I hydrates [13, 14] the $5^{12}6^2$ cage of the cubic I structure shows three inequivalent edges too. They have equal statistical weight. In addition guest molecules also populate the small isotropic 5^{12} cages and give rise to a fourth band. Since 25% of the cages are small all four sites should have equal probability $c_i = \frac{1}{4}$ for all i and the scattering function for statistical occupation of the envisaged adsorption sites is

$$\begin{aligned} S(Q,\omega) &\sim \mathrm{EISF}(Q)\delta(\omega) \\ &+ (1-\mathrm{EISF}(Q))\sum_{i=1}^{4} c_i L(\Gamma_i, \omega \pm \omega_{ti}) \\ \mathrm{EISF}(Q) &= j_0(QD) \qquad \sum c_i = 1 \end{aligned} \tag{1}$$

with Lorentzians L representing the bands of widths Γ_i at tunneling energies $\hbar\omega_{ti}$. The intensities at momentum transfer Q are fixed by the elastic incoherent structure factor EISF(Q) via the zeroth-order spherical Bessel function j_0.

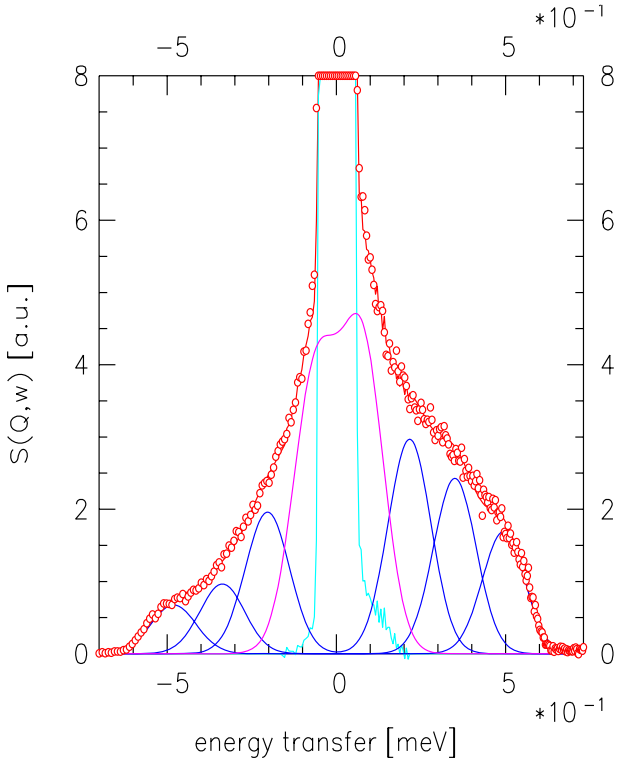

Figure 1. Spectrum of $CH_3Cl * 5.75H_2O$. Sample quenched to $T = 4.2$ K. Spectrometer: TOFTOF of FRM2, Munich. $\lambda = 6.5$ Å, $\delta E_{res} = 35$ μeV, $\bar{Q} = 1.47$ Å^{-1}. Solid lines: elastic (resolution function) and inelastic spectral components.

D is the proton–proton distance. In addition to the elastic scattering from the methyl groups there are many other sources of elastic intensity. To stabilize a fit the three outer tunnel bands were attributed identical widths. All intensities were individually adjusted to take into account deviations from thermal equilibrium due to slow and site specific spin conversion. The solid lines of figure 1 show a resolution function, the four inelastic components and the sum of all bands for the fit parameters of table 1, columns 2 and 3. (There are alternative ways to restrict the number of fit parameters such as by the assumption of a constant relative barrier height distribution function for all species [24] (see below) which will lead to slightly different parameter values.)

Intensities of energy gain and loss lines determine spin temperatures T_S of the respective tunnel system. They are slightly higher than the lattice temperature (table 1).

The integrated upscattering and downscattering intensities of different pairs of transitions are not equal as expected from the site probabilities of our model. However, the nonstoichiometry of inclusion compounds and different binding energies of different adsorption sites relax this condition. Furthermore the imposed lineshape and linewidth affect the intensities with a systematic error. A special discussion requires the high intensity of the band at the lowest energy transfer. Since its width is larger than the mean transition energy its intensity is likely greatly overestimated. A modeling in the space of rotational potentials would be more appropriate since tunneling splittings then are forced to stay on

Table 1. Ground state tunnel splittings $\hbar\omega_t$, integrated normalized intensities c_i and spin temperatures T_S based on intensities of gain and loss tunneling bands of methyl rotors in $CH_3Cl * 5.75H_2O$. On the basis of the pure threefold and sixfold potentials, mean potential strengths $\bar{V}_3$ and $\bar{V}_6$ with respective activation energies E_a are derived.

i	$\hbar\omega_t$ (μeV)	c_i	T_S (K)	$\bar{V}_3$ (meV)	E_a (meV)	$\bar{V}_6$ (meV)	E_a (meV)
1	490	0.13	6.7	3.6	2.1	18	10.6
2	345	0.18	4.6	5.9	3.6	28	17.7
3	211	0.26	6.3	9.0	5.9	42	28.4
4	70	0.43	7.8	16.0	11.6	70	51.5

one side of the elastic line [24]. While for glassy materials an accepted model of a potential distribution function exists, such a function is unknown in our case. An arbitrary choice would just give another uncertain value of the integrated intensity. Having all these problems in mind the intensities of the bands can be considered as roughly consistent with four adsorption sites of similar occurrence probabilities.

We assign the three bands at large energy transfer to methyl groups of guest molecules in the large cages and the band at the smallest energy transfers to those in the small cages. This is supported by the observation for CH_3F hydrate where this last component is fully separated from the other transitions [13].

A one-parameter rotational potential is defined just by the height of the barrier, which can for example be deduced from the tunnel splitting $\hbar\omega_t$ of the rotational ground state. Table 1 shows barrier heights of pure $\bar{V}_3$ and pure $\bar{V}_6$ potentials and corresponding activation energies. Furthermore widths δV_3 (δV_6), FWHM, of potential uncertainties can be estimated from the common linewidth $\Gamma = 73$ μeV. These widths can have different causes such as disorder of hydrogen bonds of the cage, disorder with respect to adsorption sites in neighboring cages, the presence of empty cages in the nonstoichiometric hydrate, direct interaction of guest molecules etc. It seems obvious, and calculations for methane hydrate based alone on disorder of the H bond network confirm [11], that the statistical distribution of protons in the H bonds of the cages is the main source of disorder.

A refinement of potential shapes beyond a single Fourier term requires a determination of additional rotational modes, e.g. transitions to higher levels. The spectrum measured with reduced energy resolution in a wider energy range (figure 2) shows the ground state tunnel splittings as wings of the elastic line only but resolved transitions to the second excited rotor level. Disorder affects these transitions even more than the ground state. Eight overlapping bands from four rotor systems with two transitions each, $0 \rightarrow 2$ and $1 \rightarrow 2$, smooth all details such that only a single item of information can be discussed with some confidence: transitions from the first to the second excited rotor state start at energies below $3B = 1.965$ meV. A threefold potential makes this splitting increase above $3B$. We observe the onset of transitions from the second to the third rotor level around $\sim$1.6 meV, however (figure 2). Only a strong or even dominant V_6 term which

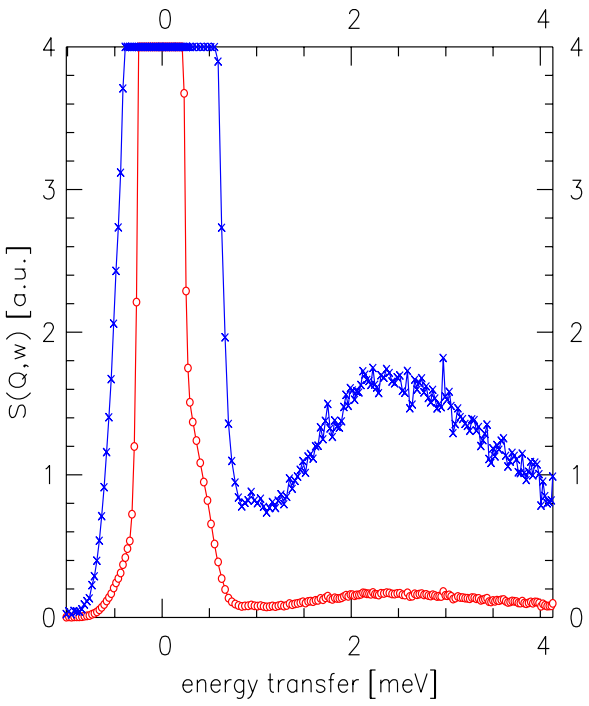

Figure 2. Spectrum of $CH_3Cl * 5.75H_2O$. The spectrum normalized to the elastic peak intensity is scaled up by factors of 200 (×) and 20 (○) to emphasize the inelastic features. Sample quenched to $T = 4.2$ K. Spectrometer: TOFTOF of FRM2. Wavelength of $\lambda = 3.8$ Å. $\delta E_{res} = 240$ μeV. Average momentum transfer $Q = 2.5$ Å^{-1}.

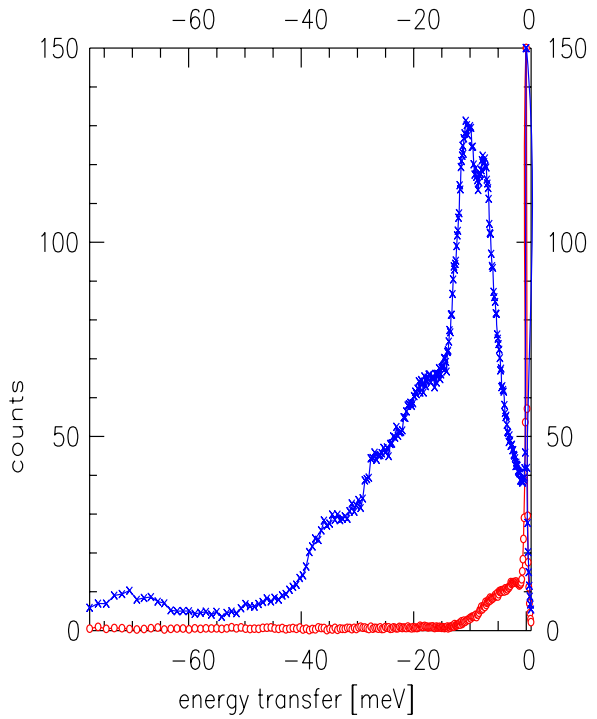

Figure 3. $CH_3Cl * 5.75H_2O$. Sample temperatures $T = 26$ K (○) and 130 K (×). Spectrometer: TOFTOF of FRM2. $\lambda = 6.5$ Å. Average scattering angle 99°.

with increasing strength unifies the four lowest levels in the rotational ground state can explain this low transition energy. A sixfold potential is in good agreement with the proposition of cage edges as adsorption sites of guest molecules. Combined with the threefold rotor symmetry, the approximate twofold site symmetry should lead to a sixfold rotational potential as already shown for $CH_3F * 5.75H_2O$ [13].

The excited rotational modes are confirmed by spectra from the time-of-flight instrument SV29 measured with an energy resolution $\delta E = 0.4$ meV.

4.2. Phonons and internal modes

Figure 3 shows the phonon spectra for energy gain of the neutron for sample temperatures $T = 150$ and 26 K. The presentation of counts versus energy transfer is chosen to keep the high energy inelastic features extending into the regime of internal modes visible. Spectra from a cold sample, $T = 2.4$ K, measured at the Jülich thermal TOF spectrometer SV29 for energy loss of the neutrons in a narrower energy range show the same doublet line at 7.4 and 10.4 meV characteristic of hydrate samples. At the low sample temperature $T = 26$ K the transition to the excited rotor level is still observable at ∼2 meV in downscattering. This shows that the quantum character of the system has to be taken into account up to rather high temperatures. Three further modes at intermediate energies of 18.1, 26.1 and 35.4 meV are clearly observed. The comparison with water spectra shows that all these energies are below the gap to internal H_2O modes and thus are likely part of the cage dynamics. Finally the band at the highest energy of 70 meV is known from pure water as the scissors mode of the H_2O molecule. These internal modes are little affected by the different crystal structures of ice and hydrate and likely contain contributions from both the molecules of the hydrate framework structure and possible contamination from pure ice crystals.

The lattice dynamics of cubic I hydrates has been measured and calculated for the cases of Xe [25, 26] and methane [27, 26] guest molecules. Theory allows us to separate modes of the guest molecules from those of the host lattice. The modes at 6.4 and 10.4 meV of a protonated host have been attributed to zone boundary translational acoustic and 'back-fold' zone center translational acoustic modes of the ice cage [27]. These modes are only slightly dependent on the type of guest and we observe them at similar energies. The assignment is confirmed by the isotopic shift towards lower energies in the deuterated host lattice measured with SV29. Lattice dynamical and single-molecule calculations would be needed to establish a more complete assignment of modes.

4.3. Quasielastic scattering

Rotation of guest molecules is the least hindered degree of freedom in hydrates. The measured large tunnel splittings are connected with low rotational barriers around the molecular symmetry axis. Therefore we base the analysis of the quasielastic spectra on methyl group rotation.

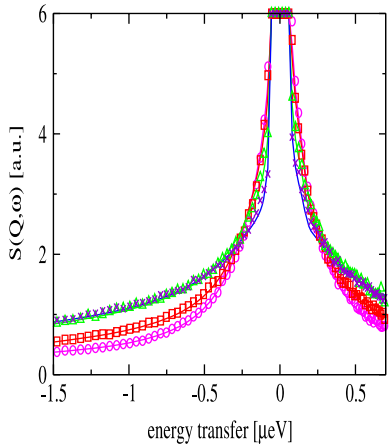

Figure 4. Temperature dependence of the quasielastic spectra of $CH_3Cl * 5.75H_2O$. Sample temperatures $T = 22$ K (○), 35 K (□), 70 K (△) and $T = 130$ K (×). Solid lines: fits with two Lorentzians. Spectrometer: TOFTOF of FRM2. Wavelength of $\lambda = 6.5$ Å. Average elastic momentum transfer $Q_{el} = 1.4$ Å^{-1}.

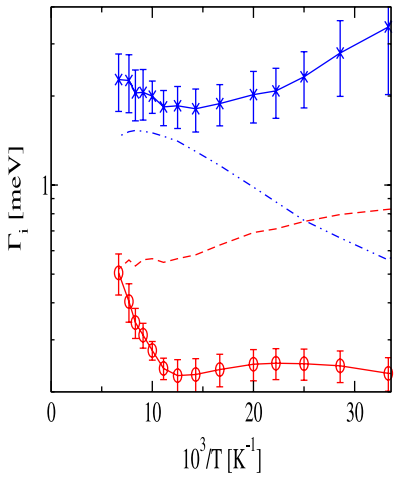

Figure 5. Temperature dependence of the widths of the two quasielastic components of $CH_3Cl * 5.75H_2O$. Symbols: linewidths. Dashed/dashed–dotted lines: corresponding intensities. Average momentum transfer $Q = 1.4$ Å^{-1}.

To separate the quasielastic scattering from the phonon background the general evolution of phonons with temperature is modeled as that of a Debye solid. The parameters are determined such that the intensity at 10.4 meV is reasonably well described at different temperatures. This means that in agreement with mathematical modeling [27] the second strong peak in the DOS is interpreted as originating from acoustic phonons. To exclude an influence of phonons not contained in this Debye description of the DOS on the parameters extracted from quasielastic intensity the fit is restricted to energy transfers from -2.2 to $+1$ meV.

From the four inequivalent methyl rotors observed in the tunneling spectrum we expect the quasielastic intensity to also contain four components. Corresponding fits occasionally abused individual Lorentzians to improve the imperfectly modeled background, indicating serious correlations of fit parameters. This shows that the system is too complex to model all its details. After many attempts the analysis of the quasielastic intensity is based on only two Lorentzians. A resolution function is added to describe the elastic line. The free parameters of the fits were the intensities and widths of the quasielastic components and the elastic intensity. The solid lines of figure 4 show fits of selected spectra. The maximum elastic intensity is ∼800 on the arbitrary intensity scale of the figure. While the general behavior is stable, the values of the fit parameters depend on the modeling of the background. Thus, the parameters are affected with a significant systematic error. Figure 5 shows the fit parameters as a function of temperature in an Arrhenius representation.

The general features of this temperature evolution can be well understood when taking into account the quantum properties of the methyl rotor. At low temperature overlapping lifetime broadened tunnel bands can be represented by a quasielastic Lorentzian whose intensity represents the sum of all tunnel bands. Obviously its width is of the order of the tunneling energies. This is the case for the narrow quasielastic component. The second component is very broad already at the lowest temperatures. This component is associated with interband transitions between the three inhomogeneously and lifetime broadened lowest rotor levels. Since the second level is around 2 meV the width of this band starts at about 2 meV. Since we only observe the energy gain side of neutrons the intensity of this band is low at low temperature and must increase with increasing temperature according to the Boltzmann population. At the same time the intensity of the narrow component must decrease with the depopulation of the rotational ground state. This interpretation is confirmed by the parameters of our modeling. We distinguish two temperature regimes in figure 5. Between $T = 30$ and ∼80 K the linewidths of the two Lorentzians are almost constant. From methane [11, 29] and methyl iodide [9] hydrates we know that the system displays the features of quantum rotation up to unusually high temperatures of ∼70 K. In this transition regime the tunnel bands broaden and simultaneously shift towards the elastic line [30]. The net result of these opposite effects is that the linewidth of a quasielastic modeling stays essentially constant. The intensity of the broad component increases almost exponentially (figure 5) as expected from a Boltzmann population. The activation energy of 3.7 meV is close to an average energy of lowest excited methyl rotational states. The slope of the decreasing intensity of the narrow component on the other hand is of the same order but with 2 meV somewhat smaller. For a sixfold rotational potential, levels at 2.1 and 3.5 meV are obtained for a potential amplitude $V_6 = 12$ meV. It does not reproduce the tunnel splitting, however, which comes out significantly larger than observed. On adding a weak threefold term the potential $(V_3; V_6) = (1; 16)$ meV leads to better consistency. This argument only emphasizes a tendency. A single average potential, especially with a single Fourier component only, is clearly too crude a simplification of the complex real situation.

Above $T \sim 80$ K the width of the narrower quasielastic line approaches an exponential increase. An Arrhenius dependence using a prefactor $\Gamma_0 = 4$ meV typical of methyl

groups yields an activation energy $E_a = 24$ meV. This value is higher than the ones estimated from the tunnel splittings for threefold potential shapes but is in the regime expected roughly for a V_6 shaped potential of the more hindered methyl rotors (table 1). This supports the same conclusion as was drawn from the low energy of the $1 \rightarrow 2$ interband transitions. The presence of a significant sixfold term in the potential expansion fits well with previous results on other methyl halide hydrates [9, 13] and supports the idea of adsorption to hydrogen bonds of the cage with their mirror symmetry.

Finally, the elastic intensity decreases weakly with increasing sample temperature according to a Debye–Waller factor. On the basis of [28] a mean square displacement $\langle u_0 \rangle^2 = 0.002$ Å^2 is derived. Since the elastic intensity is dominated by the protons and since 80% of the protons are part of the cage this low value is characteristic of the strongly bound framework atoms.

5. Conclusion

High resolution neutron scattering spectra of $CH_3Cl * 5.75H_2O$ measured at a sample temperature $T = 4.3$ K show quantum rotation of all methyl groups in weak rotational potentials. The broad structured band is the fingerprint of a complex potential surface of the ice cages with inequivalent adsorption sites. The decomposition into four subbands of comparable intensities fits well with the number and occurrence probabilities of inequivalent hydrogen bonds of the ice cage which were identified as adsorption sites already in previous studies of other methyl halide hydrates [9, 13, 14]. Proton disorder in the ice framework is the main source of the large inhomogeneous line broadening. As for many previously studied weakly hindered quantum rotor systems, the methyl rotors of the sample have not reached thermal equilibrium with the lattice temperature $T_{ph} \sim 4.3$ K. Quenching allows us to stabilize site specific spin temperatures $T_S \geqslant T_{ph}$.

Up to $T \sim 80$ K the temperature evolution of the spectra is influenced by quantum effects. An apparent quasielastic linewidth stays almost constant. Above $T \sim 80$ K, classical jump rotation determines the temperature evolution. An average activation energy $E_a = 24$ meV is derived. Methyl rotational potentials of $CH_3Cl * 5.75H_2O$ are similar to those of $CH_3Br * 5.75H_2O$. Rotational transitions to and between excited levels combined with tunnel splittings and the activation energies show the presence of a strong sixfold term in the Fourier expansion of the potential. Thus not only the number of tunneling bands but also the symmetry of the rotational potentials supports an adsorption along hydrogen bonds with their mirror symmetry.

In spite of different sizes of the $5^{12}6^2$ cages of cubic I and the $5^{12}6^4$ cages of cubic II CH_3I clathrate, the methyl rotational potentials of the two compounds are rather similar, probably since the different cages fit to the different sizes of the respective guest molecules equally well.

References

[1] Kvenvolden K A 1993 *Rev. Geophys.* **31** 17
[2] Atwood J L, Davies J E D and MacNicol D D (ed) 1991 *Inclusion Compounds* vol 5 (Oxford: Oxford University Press)
[3] Vögtle F 1992 *Supramolekulare Chemie* (Stuttgart: Teubner)
[4] Sloan E D Jr 1997 *Clathrate Hydrates of Natural Gases* 2nd edn (New York: Dekker)
[5] Gutt C, Asmussen B, Press W, Johnson M R, Handa Y P and Tse J 2000 *J. Chem. Phys.* **113** 4713
[6] Baumert J, Gutt C, Shpakov V P, Tse J S, Krisch M, Müller M, Requart H, Klug D D, Janssen S and Press W 2003 *Phys. Rev.* B **68** 174301
[7] Chazallon B, Itoh H, Koza M, Kuhs W F and Schober H 2002 *Phys. Chem. Chem. Phys.* **4** 4809
[8] Schober H, Itoh H, Klapproth A, Chihaia V and Kuhs W F 2003 *Eur. Phys. J.* E **12** 41
[9] Prager M, Pieper J, Buchsteiner A and Desmedt A 2004 *J. Phys.: Condens. Matter* **16** 7045
[10] Schweika W, Hermann R, Prager M, Persson J and Keppens V 2007 *Phys. Rev. Lett.* **99** 125501
[11] Gutt C, Press W, Hüller A, Tse J S and Casalta H 2001 *J. Chem. Phys.* **114** 4160
[12] Jeffrey G A, p. 135 of ref. [2]
[13] Prager M, Baumert J, Press W, Plazanet M, Tse J S and Klug D D 2005 *Phys. Chem. Chem. Phys.* **7** 1228
[14] Prager M, Desmedt A, Allgaier J, Russina M, Jansen E, Natkaniec I, Pawlukojc A and Press W 2007 *Phase Transit.* **80** 473
[15] Nakasako M 2002 *J. Biol. Phys.* **28** 129
[16] Press W 1981 *Single Particle Rotations in Molecular Crystals* (*Springer Tracts in Modern Physics* vol 81) (Berlin: Springer)
[17] Prager M and Heidemann A 1997 *Chem. Rev.* **97** 2933
[18] Sears V F 1966 *Can. J. Phys.* **44** 1999
Sears V F 1967 *Can. J. Phys.* **45** 234
[19] Bée M 1988 *Quasielastic Neutron Scattering* (Bristol: Hilger)
[20] Albayrak C and Zeidler M 1984 *XXIII: Congr. Ampere (Zürich)*
[21] Unruh T, Neuhaus J and Petry W 2007 *Nucl. Instrum. Methods Phys. Res.* A **580** 1414
[22] Prager M 2000 *Physica* **283** 376
[23] Krichikov A L, Gorodilov B Ya, Korolyuk O A, Manzhelii V G, Romantsova O O, Conrad H, Press W, Tse J S and Klug D D 2006 *Phys. Rev.* B **73** 064203
[24] Colmenero J, Mukhopadhyay R, Alegria A and Frick B 1998 *Phys. Rev. Lett.* **80** 2350
[25] Tse J S, Shpakov V P, Belosludov V R, Trouw F, Handa Y P and Press W 2001 *Europhys. Lett.* **54** 354
[26] Baumert J, Gutt C, Shpakhov V P, Tse J S, Krisch M, Müller M, Requart H, Klug D D, Janssen S and Press W 2003 *Phys. Rev.* B **68** 174301
[27] Tse J S, Klein M L and McDonald I R 1984 *J. Chem. Phys.* **81** 6146
[28] Trueblood K N and Dunitz J D 1983 *Acta Crystallogr.* B **39** 120
[29] Prager M 2003 unpublished
[30] Hewson A C 1982 *J. Phys. C: Solid State Phys.* **15** 3841
Hewson A C 1982 *J. Phys. C: Solid State Phys.* **15** 3855